Nuclear Inst. and Methods in Physics Research, A 924 (2019) 380–386

Contents lists available at ScienceDirect

Nuclear Inst. and Methods in Physics Research, A

journal homepage: www.elsevier.com/locate/nima

Evaluation of characteristics of Hamamatsu low-gain avalanche detectors

Sayaka Wada [a,*], Kyoji Ohnaru [a], Kazuhiko Hara [a], Junki Suzuki [a], Yoshinobu Unno [b], Koji Nakamura [b], Kazunori Hanagaki [b], Yoichi Ikegami [b], Kazuhisa Yamamura [c], Shintaro Kamada [c], Yuhei Abo [c], Hitomi Tokutake [d], Daiki Yamamoto [e]

[a] University of Tsukuba, Tsukuba, Ibaraki 3058571, Japan
[b] High Energy Accelerator Research Organization (KEK), Tsukuba, Ibaraki 3050801, Japan
[c] Hamamatsu Photonics K.K.(HPK), Hamamatsu, Shizuoka 4358558, Japan
[d] Tokyo Institute of Technology, Meguro, Tokyo 1528550, Japan
[e] Osaka University, Toyonaka, Osaka 5600043, Japan

ARTICLE INFO

Keywords:
LGAD
Avalanche
Silicon detector
Charge multiplication
4D detector
Strip sensor

ABSTRACT

Low-gain avalanche detectors (LGADs) are attractive because of their fast response to realize a 4-dimensional (4D) tracker in future experiments in high energy physics and other applications. We fabricated LGAD diodes and strip sensors. Their responses before and after irradiation to gamma rays or neutrons were evaluated with light-emitting diodes (LEDs) of various wave lengths and with an infrared laser. The sensors showed a gain of more than 10 before irradiation. Little reduction of gain was observed with gamma irradiation. A substantial reduction of gain was observed after neutron irradiation. A gain increase observed in the interstrip region after neutron irradiation, whereas the gain was equal to one before irradiation.

1. Introduction

1.1. Low-gain avalanche detector (LGAD)

The LGAD structure can be implemented in an n-in-p silicon sensor, with highly doped p^+ layer under the readout n^+ electrode. A thin layer of high electric field is created at the n^+ and p^+ junction and the signal is amplified by avalanche. A gain of approximately 10 is foreseen to be suitable for a good timing resolution as fast as 50 ps or even better [1]. A sufficient signal can be obtained with a thin detector, which allows us to reduce the sensor thickness. The density of the p^+ dopant and its thickness are key parameters as well as the thickness of the active layer and its resistivity, all of which determine the electric field hence the LGAD gain and charge collection time profile as a function of the detector bias. Here active thickness refers to the region of high resistive silicon substrate underneath the p^+ gain layer. Ultimately, we can plan to realize a 4-dimensional (4D: space and time) detector that is good for precision position and time measurement simultaneously.

1.2. Hamamatsu samples

We evaluated two types of HPK sensors: pad and strip detectors (Fig. 1). The devices were fabricated to have four different dopant densities in the p^+ gain layer. The lowest one is called "A", and the highest "D". The samples also have two different active thicknesses: 50 or 80 μm (Table 1). The pad detector that is sometimes called "monitor diode" has a circular opening of a diameter of 1 mm in the aluminum metal over the n^+ readout electrode. By shining light-emitting diode (LED) lights through the window, we characterized the devices to various wave lengths (infrared: 850 nm, red: 627 nm, green: 565 nm, blue: 464 nm).

The strip sensor has 40 strips of 10 mm length at a pitch of 80 μm, with an opening along the strip of a width of 32 μm in the 58 μm wide aluminum metal, which is connected directly to the 36 μm wide n^+ readout electrode (DC-type). By shining a laser light of a wave length of 1064 nm, we measured charge collection and evaluated the gain and its uniformity across the strips. The diodes were irradiated to gamma and neutron sources, and the strips to neutrons (see Section 2.3 for details) and were characterized before and after irradiation.

2. Electrical properties

2.1. Monitor diode I–V curve

Fig. 2(a) and (b) show the current versus bias voltage (I–V) characteristics measured for the 80D diode illuminated by the LEDs with various wavelengths. The LED intensities were adjusted to equalize the currents at 10 V. There is a jump in IV curves between 20 and 35 V

* Corresponding author.
E-mail address: wada@hep.px.tsukuba.ac.jp (S. Wada).

https://doi.org/10.1016/j.nima.2018.09.143
Received 5 March 2018; Received in revised form 17 September 2018; Accepted 27 September 2018
Available online 5 October 2018

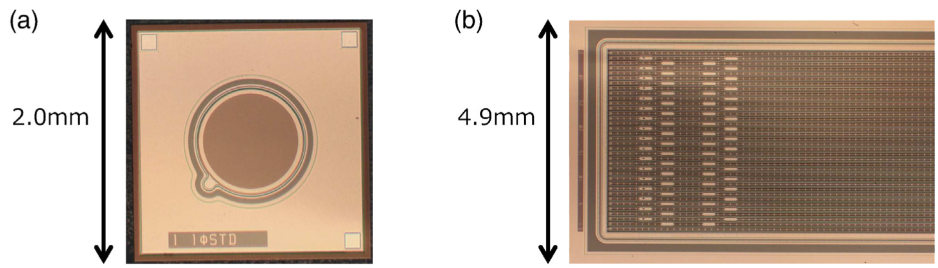

Fig. 1. Photos of pad (a) and strip (b) detectors.

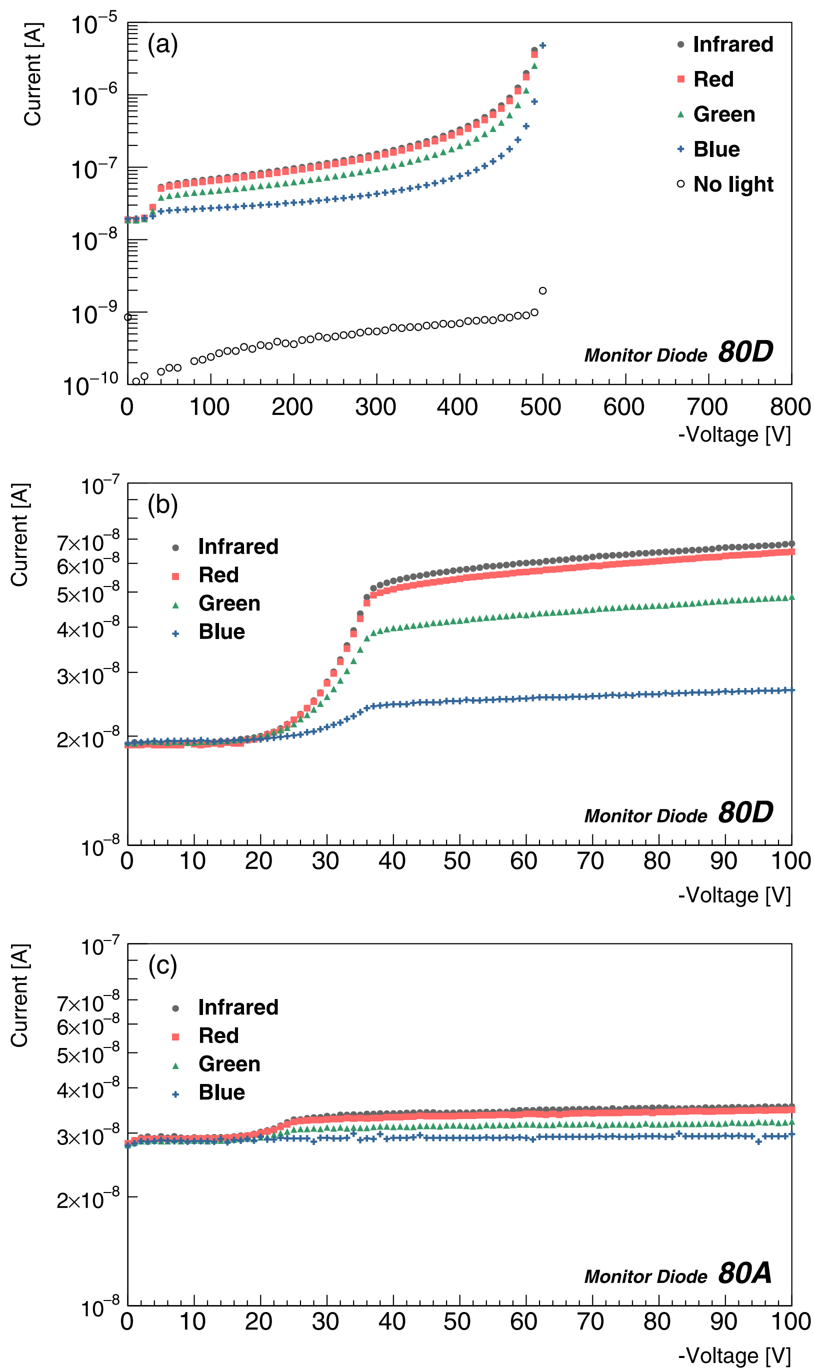

Fig. 2. Leakage current versus bias voltage measured at 20 °C with illumination by various LED lights for monitor diode; (a) 80D up to 500 V, (b) same data as (a) but expanded up to 100 V and (c). 80A up to 100 V.

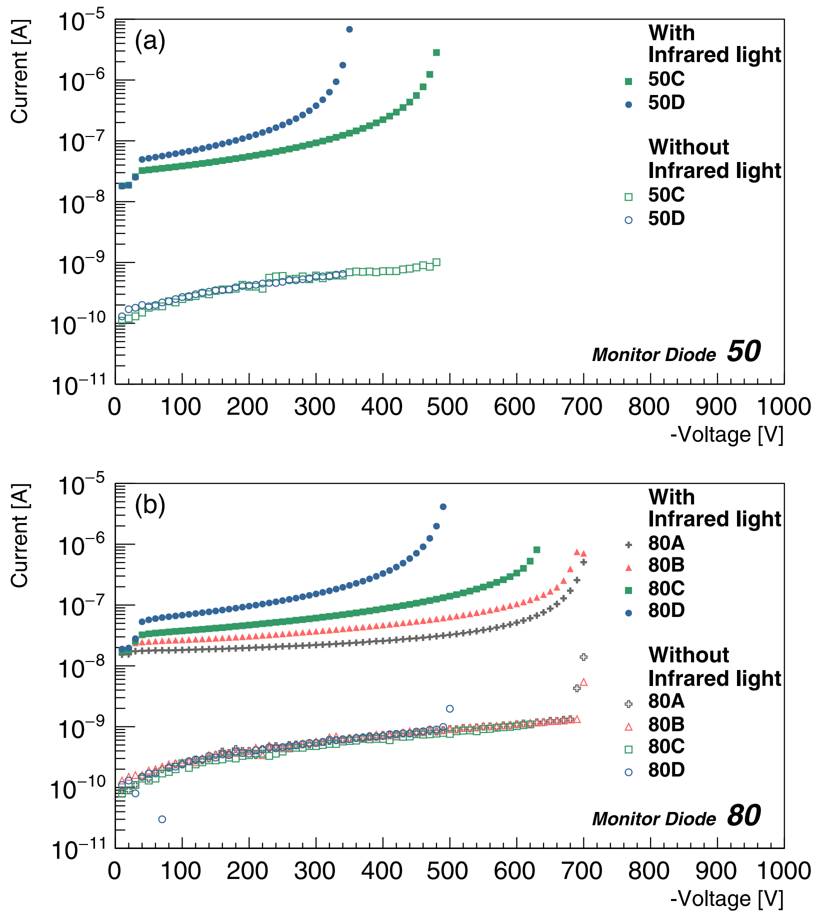

Fig. 3. Leakage current versus bias voltage measured at 20 °C with and without illumination by an infrared LED for monitor diode of (a) 50 μm active thickness and (b) 80 μm active thickness.

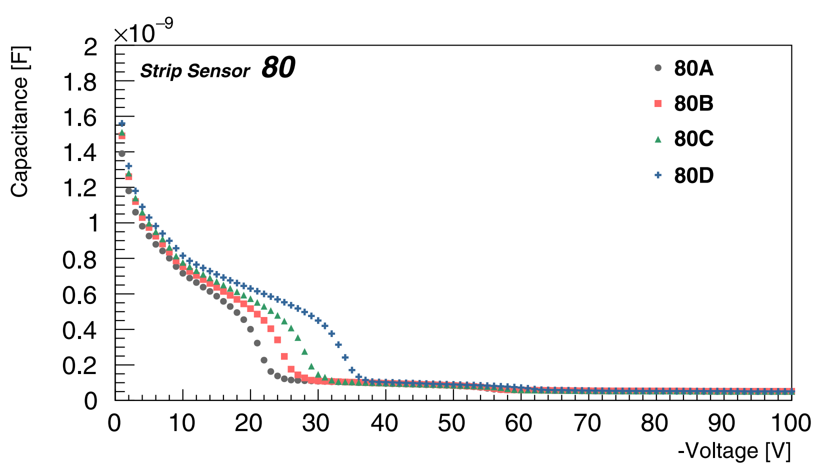

Fig. 4. C–V curves at 20 °C for strip 80 μm thick sensors with different p^+ dopant densities.

that corresponds to the depletion of the active layer. The magnitude of the jump depends on a wavelength of a photon, photons with longer wavelength penetrate deeper and generate more current. Fig. 3 shows I–V curves for the other diode samples with and without infrared light. A larger current caused by avalanche amplification is observed for the devices with a higher p^+ dopant. From these observations, the p^+ density of the C and D types for 50 μm samples and D type for 80 μm is suitable for larger amplification achievable at manageable bias voltage (typically less than 500 V before irradiation).

2.2. Bulk capacitance

Fig. 4 shows the capacitance versus bias voltage (C–V) curves of the strip sensor with 80 μm active thickness. For bias voltages in the range 0–10 V, the capacitance drops rapidly, and then for bias voltages up to 30 V, it drops slowly depending on the p^+ density. The capacitance further drops rapidly again for bias voltages above 30 V. The first part, below 10 V, corresponds to the depletion sideway between strips, and the second part, 10–30 V, to the depletion of the p^+ layer. The last part corresponds to the depletion of the bulk. The full depletion voltages of

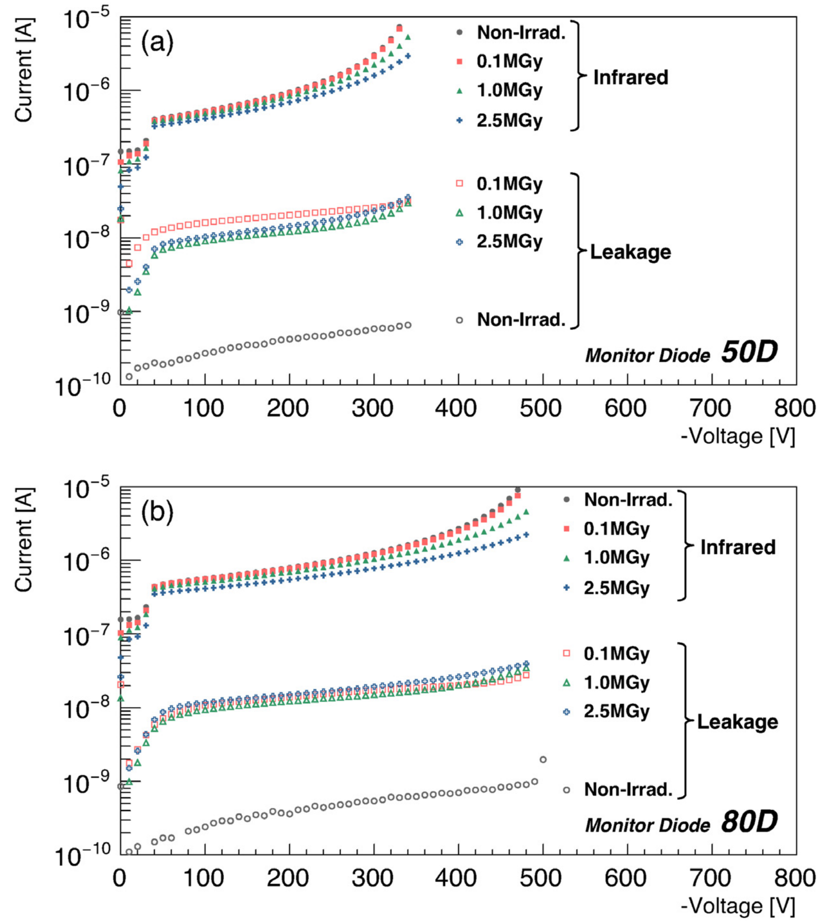

Fig. 5. I–V curves after γ-ray irradiation for monitor diodes: (a) 50 μm active thickness and (b) 80 μm active thickness. Non-irradiated/irradiated samples were characterized at 20/−20 °C, respectively. The I–V curves denoted as leakage with light off, while those as Infrared are with LED light (leakage subtracted).

Table 1
Sample list of HPK LGAD samples.

Sample name	p^+ dose low to high	Physical thickness [μm]	Active thickness [μm]
50A	A	150	50
50B	B		
50C	C		
50D	D		
80A	A		80
80B	B		
80C	C		
80D	D		

25 to 35 V are in agreement with the I–V results as shown in the previous section.

2.3. Radiation tolerance

The surface and bulk radiation damages were investigated with γ-rays and neutrons, respectively. The ^{60}Co γ-ray irradiation was performed at Takasaki Advanced Radiation Research Institute in Japan [2]. The irradiation doses were 0.1, 1.0, and 2.5 MGy. Fig. 5 shows the dark current and the current induced by the infrared LED for irradiated and non-irradiated 50D and 80D samples. In all samples, the dark current increased but the avalanche amplification is not degraded significantly by gamma irradiation as compared to the neutron irradiation as described below.

The neutron irradiation was performed at the Ljubljana reactor in Slovenia [3]. The irradiation fluences were (0.3, 1.0, 3.0) × 10^{15} 1-MeV n_{eq}/cm^2. Fig. 6 shows the response to the infrared light measured after annealing for 80 min at 60 °C [4]. The amplification dropped and required a higher voltage to retain the same amplification value. We confirm that types C and D showed higher amplification at lower bias voltage than types A and B, and the active thickness of 50 μm than of 80 μm.

3. Gain evaluation

We measured the charge collection for the strip sensor with the Alibava system [5]. We used a pulsed infrared (IR)-laser (Nd:YAG) of wavelength 1064 nm, focused at the surface of the device and collimated to a region of 2 × 2 μm^2. A collective effect of photons from the laser beam mimics a charged particle traversing the sensor, generating electron–hole pairs uniformly along depth.

Fig. 7 shows the collected charge for different values of the bias voltages of the non-irradiated strip sample (50D) when the laser was injected at the center of strip (Fig. 7(b)) and in the interstrip region (Fig. 7(a)). The tendency that the gain in the interstrip region stays constant is observed also for 80D sample. The collected charge stays constant and does not depend on the bias voltage in the interstrip region, hence there is no charge amplification and the gain is equal to 1, as expected. Therefore we use the collected charge in the interstrip region to define the gain in the entire region across the strip. We defined the gain of the strip sensor by the most probable value of ADC distribution normalized by that of the non-irradiated sample measured at the interstrip region and at 50 V bias:

$$\text{Gain (V)} = \frac{\text{ADC\_center (V)}}{\text{ADC\_interstrip (50 V; non-irradiated)}}.$$

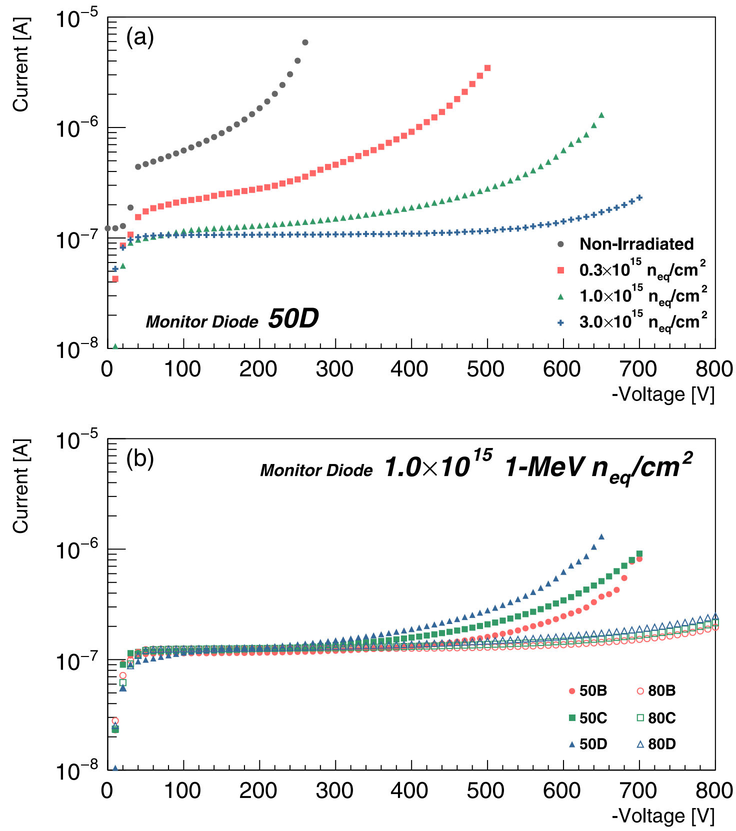

Fig. 6. I–V curves of 50D measured at −40 °C illuminated by infrared LED (leakage subtracted) for different neutron fluence (a) and diodes with different p$^+$ densities irradiated to 1.0×10^{15} 1-MeV n_{eq}/cm^2 (b).

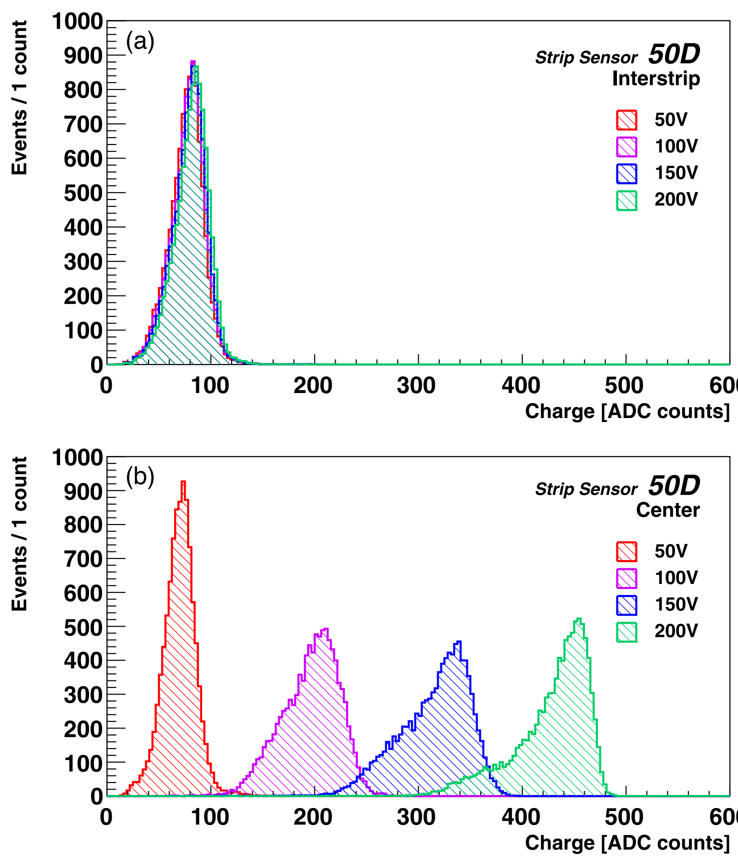

Fig. 7. Charge collection of non-irradiated strip sensor: (a) in the interstrip region and (b) at the center of strip, measured at 20 °C.

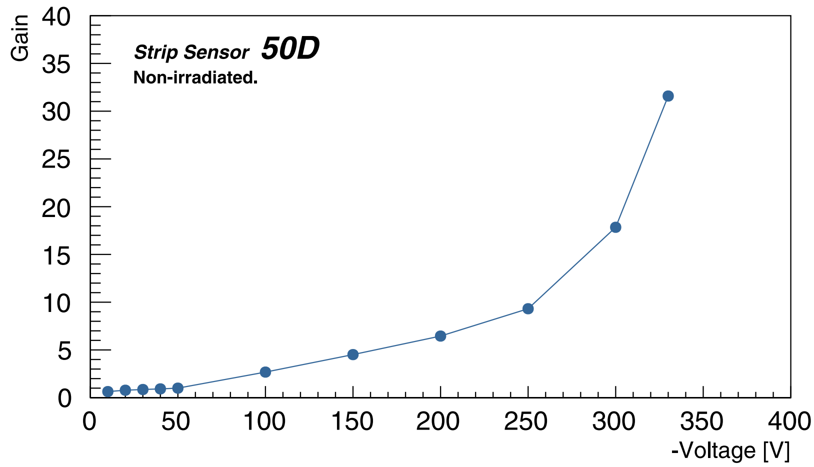

Fig. 8. Gain at the center of a strip as a function of the bias voltage for non-irradiated sample.

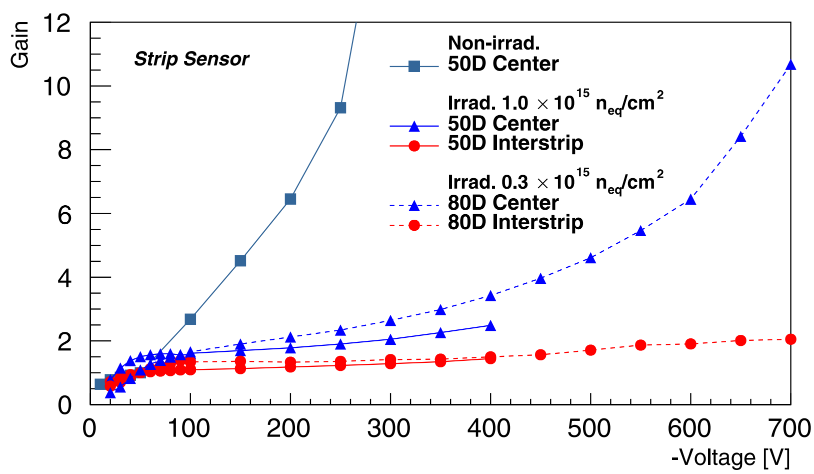

Fig. 9. Gain at the center of strip and in the interstrip as a function of the bias voltage for 0.3 (80D, dashed curves) and 1.0 (50D, solid curves) $\times 10^{15}$ 1-MeV n_{eq}/cm^2 neutron irradiated samples. The non-irradiated sample is also plotted for comparison.

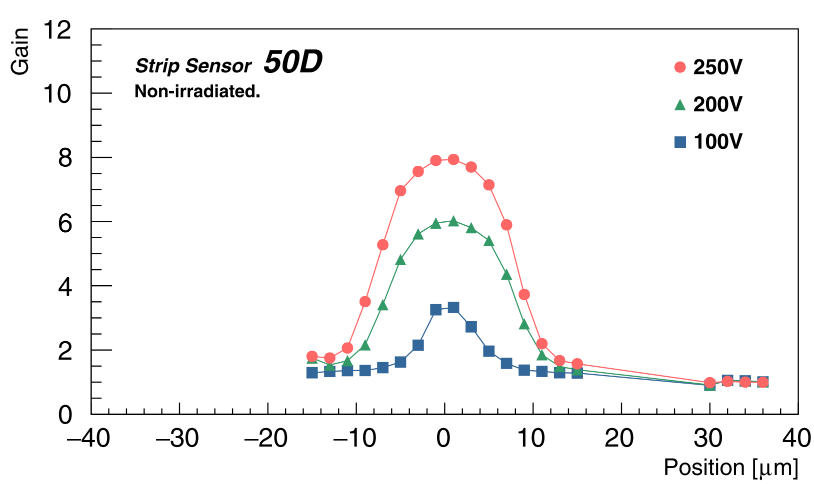

Fig. 10. Collected charge dependence on location across a strip (non-irradiated). The strip center is located at 0. The region (16 – 28 μm) is covered with aluminum connected to the n^+ electrode.

Gain as a function of bias voltage is shown in Fig. 8. A gain of approximately 30 was obtained at 330 V, which is a gain suitable for LGAD application.

We also measured the charge collection of the samples irradiated to 0.3 and 1.0×10^{15} 1-MeV n_{eq}/cm^2 after the annealing treatment. As the collected charge did not change up to 400 V in the interstrip region, the gain was set to 1 at 50 V as for the non-irradiated sample, and the gain in the center region was calculated according to the equation given above (Fig. 9). A gain of 10 was obtained at 700 V for 80D at 0.3×10^{15} 1-MeV n_{eq}/cm^2. As we expect a larger gain for 50D than

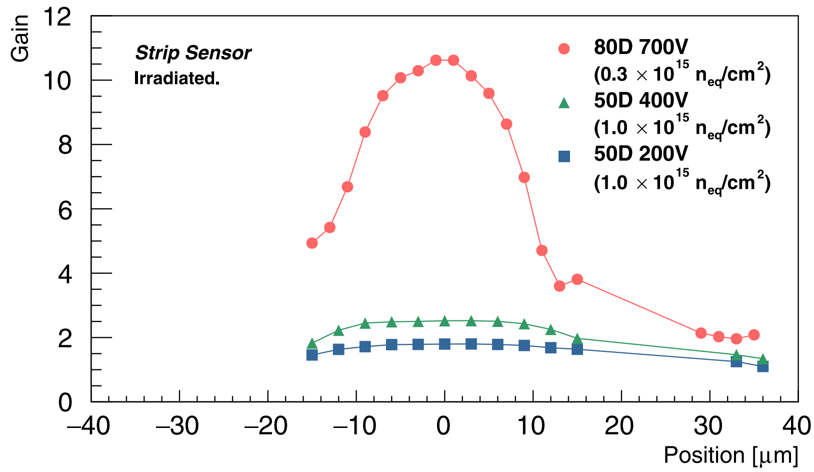

Fig. 11. Collected charge dependence on location across a strip (irradiated); 80D irradiated to 0.3×10^{15} 1-MeV n_{eq}/cm^2 and 50D to 1.0×10^{15} 1-MeV n_{eq}/cm^2. The strip center is located at 0. The region (16 - 28 μm) is covered with aluminum connected to the n^+ electrode.

80D at the same voltage, the gain reduction from 80D to 50D irradiated samples implies that the gain was reduced significantly, more than a factor of two at 400 V, from 0.3 to 1.0×10^{15} 1-MeV n_{eq}/cm^2. A possible interpretation of the gain reduction is change of the p+ active density due to the acceptor removal [6,7].

Fig. 10 shows the dependence of the gain on the location of laser injection across the strip of non-irradiated strip sample at the bias voltages up to 250 V. The gain is maximum in the strip center and drops towards the edges of the strip. The shape of the gain dependence on the location seems to stay similar above 200 V. The laser spot size is very small, therefore the gain drop should be related to the structure and/or the applied voltage. The extension of the gain fully to the edges is final our goal and is a subject to be investigated further.

The same distribution as on Fig. 10 is shown on Fig. 11 for the irradiated sample to neutron fluence of 1.0×10^{15} 1-MeV n_{eq}/cm^2. The gain of 10 was observed for 80D at a bias voltage of 700 V at the center of strip. For 80D sample the gain in the interstrip region is about 2 at 700 V for irradiated sample while for non-irradiated the gain was equal to one. This is an indication that the electric field at the edge of the n+ strip is high enough to induce an avalanche breakdown, when the high bias voltage applied, in the irradiated sample.

4. Conclusion

We have fabricated n-in-p LGAD pad and strip sensors with four densities of p^+ gain layer and two thicknesses of active volume. We found that a larger amplification was achieved in a device with a thinner active thickness (50 μm) and a higher p^+ density. A gain of approximately 30 was reached for the non-irradiated sample. The gain varied little with gamma irradiation up to 2.5 MGy. The gain dropped substantially after neutron irradiation. With a strip-type (DC coupled) LGAD sample, we evaluated the gain dependence on the location across strip. In the strip region, a gain of 10 was reached before, as well as after neutron irradiation to 1.0×10^{15} 1-MeV n_{eq}/cm^2. In the interstrip region, a gain of 1 before and 2 after irradiation was observed.

The basic LGAD characteristics especially for the strip type provides useful information for designing segmented devices, which is an ultimate goal to realize 4D tracking in particle physics experiments.

Acknowledgments

The neutron irradiations were performed at Ljubljana, supported by AIDA-2020, CERN/EU Grant Agreement no. 654168.

References

[1] H.F.-W. Sadrozinski, A. Seiden, N. Cartiglia, 4d tracking with ultra-fast silicon detectors, Rep. Progr. Phys. 81 (2018) 026101.
[2] L. Snoj, G. Zerovnik, A. Trkov, Computational analysis of irradiation facilities at the jsi triga reactor, Appl. Radiat. Isot. 70 (2012) 483–488.
[3] Takasaki Advanced Radiation Research Institute, National Institutes for Quantum and Radiological Science and Technology, homepage; www.taka.qst.go.jp/tiara/665/english/index_e.php.
[4] M. Moll, Radiation Damage in Silicon Particle Detectors Hamburg University (Ph.D. thesis), 1999.
[5] R. Marco-Hernandez, A portable readout system for microstrip silicon sensors (alibava), IEEE Trans. Nucl. Sci. 56 (3) (2009).
[6] S. Terada, et al., Proton irradiation on p bulk silicon strip detectors using 12 gev ps at kek nucl, Instr. Meth. A 383 (1996) 159–165.
[7] G. Kramberger, Radiation Effects in Low Gain Avalanche Detectors After Hadron Irradiations, in: JINT, vol. 10, 2015, p. P07006.